Current Chemistry Letters 13 (2024) 303–314

Contents lists available at GrowingScience

Current Chemistry Letters

homepage: www.GrowingScience.com

Molecular docking, elucidating the regiospecificity and the mechanism of [3+2] cycloloaddition reaction between azidobenzene and propiolaldehyde

Kamal Ryachi[a,b], Ali Barhoumi[b], Mhamed Atif[a], Aslı Eşme[c], Abdessamad Tounsi[a], Mohammed El idrissi[d*] and Abdellah Zeroual[b*]

[a]*Agro-industrial, Environmental and Ecological Processes Team, Faculty of Science and Techniques of Beni Mellal, Sultan Moulay Slimane University, Beni Mellal, Morocco*
[b]*Molecular Modelling and Spectroscopy Research Team, Faculty of Science, Chouaïb Doukkali University, P.O. Box 20, 24000 El Jadida, Morocco*
[c]*Department of Elementary Science Education, 41380, Umuttepe, Kocaeli, Turkiye*
[d]*Team of Chemical Processes and Applied Materials, Faculty Polydisciplinary, Sultan Moulay Slimane University, Beni-Mellal, Morocco*

C H R O N I C L E

Article history:
Received March 20, 2023
Received in revised form
June 17, 2023
Accepted December 12, 2023
Available online
December 12, 2023

Keywords:
6LU7
MEDT
Regiospecific
Azidobenzene
ELF
Propionaldehyde

A B S T R A C T

Molecular electron density theory has been performed with the B3LYP/6-31(d,p) method to study the [3+2] cycloaddition processes between azidobenzene and propionaldehyde, the reactivity indices, activation and reaction energies are computed. The reaction and activation energies indicate that this [3+2] cycloaddition reaction is regiospecific, in good agreement with the experimental results. ELF examination revealed that the mechanism of these cycloaddition reactions takes place in two steps. In addition, a docking approach was performed on the products investigated, and the interaction with the protein protease COVID-19 (PDB ID: 6LU7), the results confirm that the presence of triazole and isoxazole rings increases the affinity of these products.

1. Introduction

Triazoles are five-membered heterocyclic compounds containing three nitrogen atoms and two carbon atoms[1] (Fig. 1). Triazoles are often used as ligands in coordination chemistry and catalysis, as well as in organic synthesis for the formation of carbon-nitrogen bonds and are often synthesized using the nitrogen-alkyne cycloaddition reaction[2] and are also present in some drugs and in compounds with interesting biological properties, such as antimicrobial, antiviral and anticancer properties[3]. These properties have led to studies on the potential of triazole as a drug candidate in the treatment of various diseases. Another family of heterocyclic organic compounds is the isoxazoles, which have one oxygen atom and one nitrogen atom in the ring (**Fig. 1**). 2-isoxazoline has applications in pharmaceutical and agrochemical chemistry[4]. They can be used as precursors in the synthesis of other heterocyclic compounds and are used as herbicides and fungicides in agriculture, they also have applications in the synthesis of drugs and pharmaceuticals, and have been studied for their analgesic, anti-inflammatory and antinociceptive properties[5], isoxazoles can be prepared by cycloaddition reactions between nitrilroxides and alkenes[6] (**Fig. 1**).

* Corresponding author.
E-mail address zeroualabdellah2@gmail.com (A. Zeroual), M. El idrissi

doi: 10.5267/j.ccl.2023.12.002

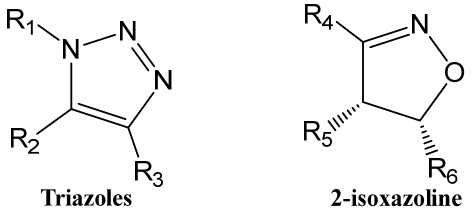

Fig. 1. Triazoles and isoxazoles structures

The computerized method known as DFT (Density Functional Theory) in physics and chemistry is used to characterize the electrical properties of molecules, materials, and surfaces[7]. The strategy was created using the quantum theory of matter, which characterizes subatomic particles in terms of waves and wave functions. Within the framework of the DFT method another theory has recently been proposed called MEDT, which is very good at predicting the electrical and physical properties of the chemical structures. It is commonly used for modeling chemical reactions in addition to predicting chemical reactivity[8]. This concept has been applied in several surveys to explain how reactive cycloaddition mechanisms work[9-20].

In order to understand the processes and the selectivity of the cycloadditions reactions mentioned in **Scheme 1**, the MEDT has been used technique to explore the selectivity and mechanism of these [3+2] cycloadditions reactions[21].

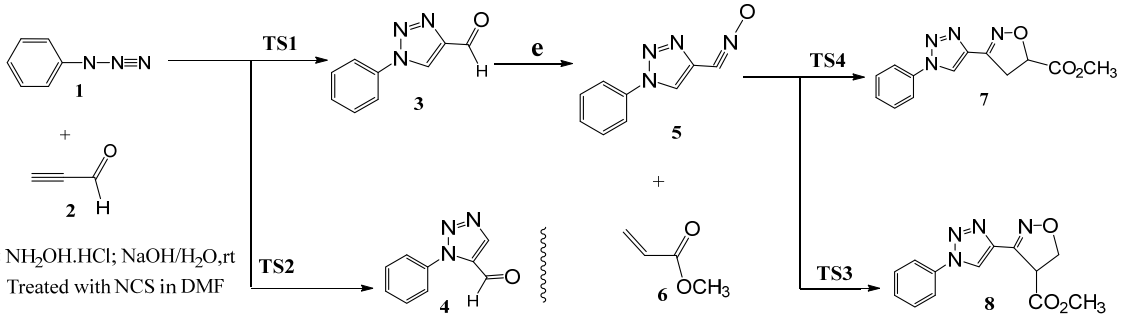

Scheme 1

2. Computation Methodology

B3LYP is a functional approach in DFT theory which has been applied to describing the electrical and energetic properties of molecular structures[22]. Basis 6-311(d,p) has been applied to study electron distribution in molecules[23]. All calculation processes are performed in Gaussian 09[24]. The transition states (TS) were identified and verified through the existence of a singular imaginary frequency. The IRC also helps to evaluate the reaction trajectory from its initial to final state, and to understand the intermediate steps and the activation barriers attached to them. Tomas' PCM has been used to take the solvent's impact on the optimized structures into account. (Polarizable Continuum Model)[25-30]. The electronic chemical potential is a thermodynamic measure that indicates the tendency of a reactant to gain or lose electrons from its electronic structure, and it is described as follows: $\boldsymbol{\mu} = \frac{E_L + E_H}{2}$. Chemical hardness is a concept from chemistry describing a molecule's resistance to disorder in its electronic structure, which is defined by the relationship: $\eta = E_L - E_H$, based on the energies of the HOMO and LUMO boundary molecular orbitals, expressed as: E_H and E_L.

The measure designated global electrophile index (w) is a quantity used in chemistry to appreciate the capacity of a molecule to intervene as an electrophile, in other terms to capture electrons from other molecules to establish a chemical bond, and is explained by the formula below: $\omega = \frac{\mu^2}{2\eta}$ [31], Furthermore, in opposite to the electrophile index, the nucleophile index (N) is a useful measure of a molecule's capacity to behave as a nucleophile, i.e. to donate electrons to another molecule to create a chemical bond, which is given as follows: $E = E_{HOMO}$ (Nu)-E_{HOMO} (TCE)[32].

Parr functions are used to calculate local indices, which are fundamental spin functions in quantum chemistry to describe the distribution of electron spins in molecules[33,34]. The electron localization function is based on the Topmod program (ELF)[35,35].

3. Results and discussion

3.1. Analysis of the CDFT indices for reagents

Numerous investigations on chemical reactions[25-30] have shown that evaluating the reactivity indices provided inside CDFT is an efficient method for assessing the reactivity of organic molecules. In order to forecast the reactivity of phenylazide (**1**), propiolaldehyde (**2**), nitrile-oxide (**5**) and methyl-acrylate (**6**) in the cycloadition processes, the global indices electrophile, nucleophile, chemical hardness, and electronic chemical potential are explored in **Table 1.**

Table 1. Values of phenylazide (**1**), propiolaldehyde (**2**), nitrile-oxide (**5**) and methyl-acrylate (**6**), as determined by B3LYP/6-31G(d), in terms of nucleophile N, electrophile, electrochemical potential, and chemical hardness; all values are in electron volts (eV).

System	η	μ	ω	N
1	5.16	-3.62	1.26	3.32
2	5.53	-4.80	2.08	1.96
5	4.91	-4.00	1.62	3.07
6	6.16	-4.31	1.50	2.13

While the disparity in chemical electron potentials suggests[37] that this cycloaddition reaction is polar, the chemical electron potential of 1 (μ = -3.62 eV) is lower than that of 2 (μ = -4.80 eV), suggesting to an electro-flow from **1** to **2**, on the other hand 5's chemical electron potential (μ= -4.00 eV) is lower than that of 6's (μ= -4.31 eV), reveals that there is an electro-flow from **5** to **6**, although the difference in chemical electron potential indicates that this cycloaddition reaction between 5 and 6 is non-polar. The electrophile index ω[38,39] and nucleophile index N[35] of **1** (1.26 and 3.32 eV) and for **5** are (1.62 and 3.07 eV) respectively, and therefore its classification in the families of strong electrophiles and strong nucleophiles. The electrophile index ω of **2** and 6 are (2.08, 1.50 eV) respectively, which classifies it as a strong electrophile, and the nucleophile index N are (1.96, 2.13 eV), respectively, which classifies it as a moderate nucleophile according to the standard electrophile[39] and nucleophile scales[40], Inferring that whereas **2** and **6** will act as electrophiles in this reaction, **1** and **5** will participate as nucleophiles.

3.2. Local indices

Since their introduction by Luis Domingo[41], Parr functions are used extensively in theoretical chemistry to predict the chemical reactivity of organic compounds. Several studies show that first bonding is established on the center with the highest Parr electrophylic value in dienophiles. Figure 2 displays the electrophilic Parr functions of the two dienophiles, **2** and **6**.

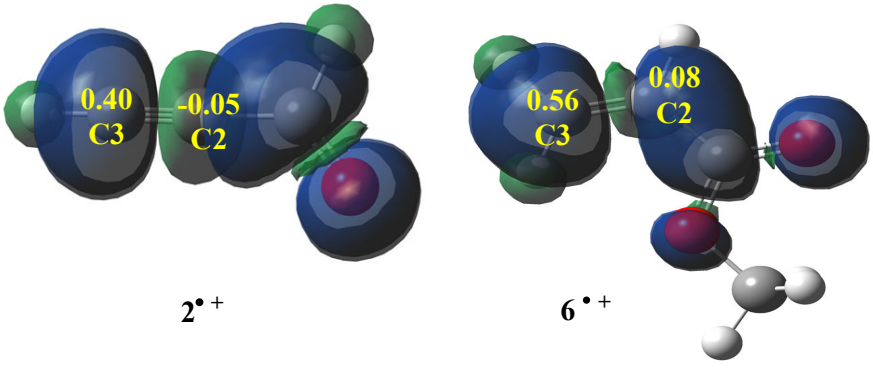

Fig. 2. The electrophilic Parr functions with 3-dimensional atomic spin density (ASP) mappings of the reagents **2** and **6**.

Fig. 2 reveals that the Mulliken atomic spin densities of propiolaldehyde (**2**) $P_3^+ = 0.56$ and methyl-acrylate (**6**) $P_3^+ = 0.40$, are highly localised on the C3 centre of both molecules, while there is almost no surface area around the C2 centre. This result indicates that the C3 center is the most reactive, so the first bond will form on the C3 center of propiolaldehyde (2) and methyl-acrylate (6).

4. ELF studies of reagents

The Electron Localization Function (ELF) is a technique used in quantum chemistry and solid-state physics to analyze the electronic structure of molecules. The ELF is a function that provides information about the degree of electron localization within a given region of space. The ELF can be used to identify the nature of chemical bonds within a molecule. For example, a high ELF value in a certain region indicates the presence of a covalent bond, while a low ELF value indicates

the absence of a bond or the presence of a weakly interacting species. The ELF basins for the reactants and the attractor are assigned in **Fig. 3** at their important positions.

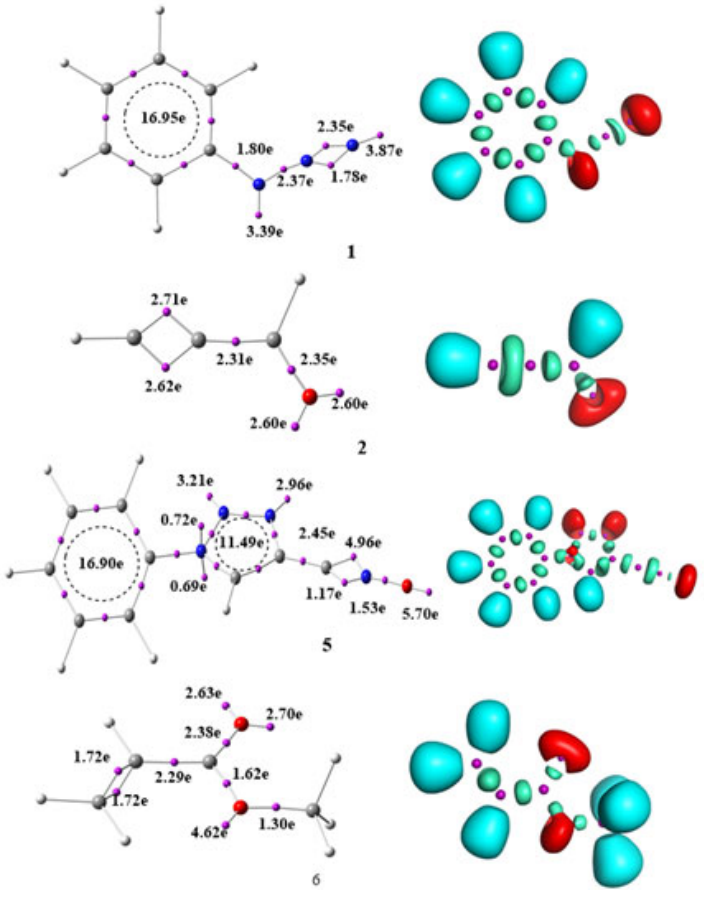

Fig. 3. B3LYP/6-31G(d,p), ELF positions basin attractors with ELF localization domains with the greatest relevance for valence basin populations are described at an ELF isosurface value of 0.80, of phenylazide (**1**), propiolaldehyde (**2**), nitrile-oxide (**5**) and methyl-acrylate (**6**), the average number of electrons.

The two free pairs of non-bonding electrons on the N1 and N3 nitrogen atoms are shown to be associated with a single monosynaptic basin V(N1) and V(N3) that has an electron population of 3.39e and 3.87e, respectively, in the phenylazide (**1**) ELF building design. The existence of two disynaptic clusters V(N2,N3) and V'(N2,N3) with a cumulative electron population of 4.13e indicates the presence of an N2=N3 double bond, while the N1-N2 bonding region exhibits a significant double bond nature due to the presence of a disynaptic cluster V(N1,N2) with an electron population of 2.13e. Because of the 37e electron population, this structure suggests that BAZ 1 participates in the cycloaddition reaction between phenylazide (1) and propiolaldehyde (2) in the form of a pseudodiradical.

It can observed in propiolaldehyde (**2**), existence of two disynaptics pools V(C2,C3) and V'(C2,C3) which have a total electron population of 5.33e, one disynaptic pool V(C1,C2) integrating 2.31e and existence of two monosynabtics carried by the oxygen atom of value 5.20e.

In molecule 6 we observe essentially two bisynaptic basins between carbons C2 and C3 integrating in total VT(C2,C3)=3.42e, in reagent 5, we observe the presence of a monosynaptic basin around the oxygen atom of value 5.70e and two bisynaptic basins between carbon C1 and the nitrogen atom of total value 6. 13e, which shows the existence of a triple bond between the carbon C1 and the nitrogen atom, another bisynaptic basin located between the nitrogen atom and the oxygen atom with a value of 1.53e, this electronic distribution clearly shows that nitrile oxide will participate in the cycloaddition reaction between nitrile-oxide (5) and methyl-acrylate (6) as a zwiterionic type.

5. Energetical considerations

Phenylazide (1), propiolaldehyde (2), nitrile oxide (5) and methyl acrylate (6) are non-symmetrical reactants, so the [3+2] cycloaddition reaction between phenylazide (1) and propiolaldehyde (2) will lead to two pathways and the [3+2] cycloaddition reaction between nitrile oxide (5) and methyl acrylate (6) will provide two other pathways, so in this study

there are four pathways in total (Scheme 2). The thermodynamic values are providing in table 2 and the geometries of the transitions states are displayed in Figure 4.

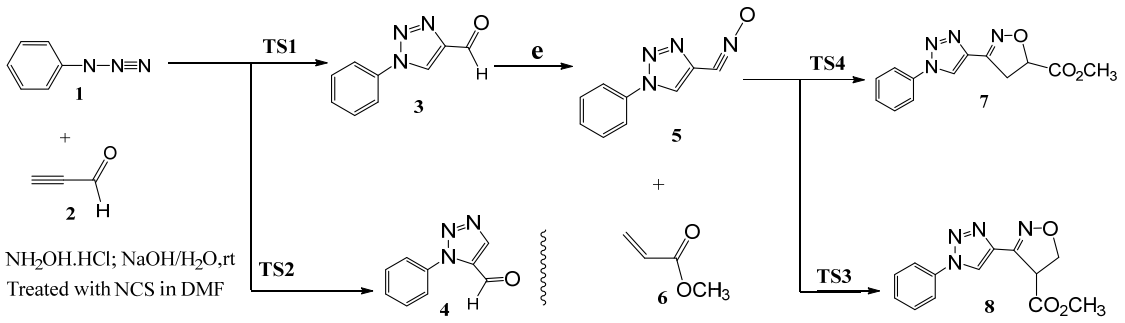

Scheme 2 Competitive reaction pathways involved in the 32CA reaction between 1 and 2 [5+6].

Table 2. B3LYP/6-31(d,p) relative (ΔE, ΔH and ΔG, in kcal-mol^{-1}) energies, in DMSO, for the species involved in the opening of the cycloaddition reaction between 1+2 and between 5+6.

System	ΔE	ΔH	ΔG	ΔS
1	-------	-------	-------	-------
2	-------	-------	-------	-------
1+2	-------	-------	-------	-------
TS1	**15.5**	**15.9**	**27.6**	**-39.268**
3	**-73.8**	**-70.0**	**-55.3**	**-48.989**
TS2	**16.6**	**16.9**	**29.1**	**-40.843**
4	**-70.5**	**-66.7**	**-52.1**	**-48.939**
5	-------	-------	-------	-------
6	-------	-------	-------	-------
5+6	-------	-------	-------	-------
TS3	**12.8**	**13.2**	**26.5**	**-44.527**
8	**-38.5**	**-35.4**	**-21.4**	**-46.981**
TS4	**11.1**	**11.5**	**23.6**	**-40.566**
7	**-39.1**	**-36.3**	**-48.8**	**-46.982**

Analysis of the relative energies of the stationary points involved in the 32 CA reaction between phenylazide (1) and propiolaldehyde (2), leads to some interesting conclusions: (i) the most favorable TS1 is found at 15.5 Kcal·mol^{-1} below the separate reactants and TS2 is found at 16.6 kcal-mol-1 below the separate reactants; (ii) this 32CA reaction is highly exothermic at 73.8 Kcal·mol^{-1} for product 3 and 70.5 for product 4. Therefore, the formation of product 3 occurs by kinetic and thermodynamic control. (iii) this 32CA reaction is completely ortho-regioselective, as TS2 is found to be 1.1 Kcal·mol^{-1} higher than TS1.

Some intriguing findings are drawn from an analysis of the relative energy of the stationary points involved in the 32CA reaction between nitrile-oxide (**5**) and methyl-acrylate (**6**):

(i) The preferable TS4 appears at 11.1 Kcal·mol^{-1} under the separate reactant and the most favorable TS3 is discovered at 12.8 Kcal·mol^{-1} below the separate reactants.

(ii) (ii) this 32CA reaction is exothermic at 39.1 Kcal·mol^{-1} for product 7 and 38.5 for product 8. Therefore, kinetic and thermodynamic control governs the creation of product 3.

(iii) (iii) Given that TS4 has been found to be 1.1 Kcal·mol^{-1} bigger than TS3, this 32CA reaction is entirely ortho-regioselective.

The geometries of the four TSs are illustrated in Figure 4. At the most favourable ortho TSs TS1 and TS4, the distances between the N1-C3 and C2-N3 interacting centers are 2.031 and 2.356 Å at TS1 and 2. 171 and 2.439 Å at TS4, while at the meta TSs, the distances between the two interacting centres C3-N3 and C2-N1 are: 2.060 and 2.314 Å, respectively, at TS2 and 2.190 and 2.285 Å, respectively, at TS3.

These distances indicate that the most favourable TS1 and TS4 have high geometric asynchronism respectively Δl=0.324 and Δl=0.268 Å, the most unfavourable TS2 and TS3 have very low geometric asynchronism respectively Δl=0.254 and Δl=0.095 Å [42].

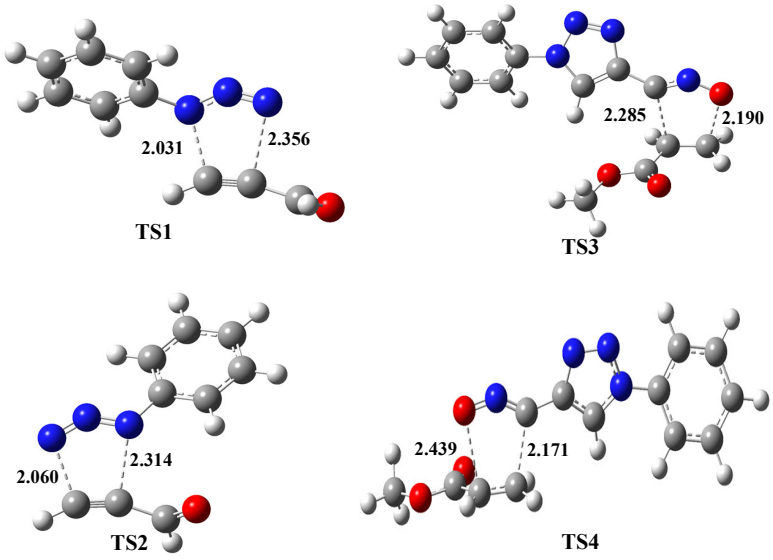

Fig. 4. B3LYP/6-31G(d,p) geometries of the optimized transition states associated with the 32CA reactions between 1 and 2 (5 and 6), distances are given in Angstrom, Å.

6. Bond evolution theory study

The mechanism of a reaction can be investigated using an electron localization function (ELF). We can track variations in electron density (electron population) along the chemical route by applying ELF to the IRC profile. This enables a thorough mechanism analysis of the reaction by allowing us to determine precisely when a given bond is being produced or broken and to investigate the interchange of the electron population in lone pair atoms and in bonds.

6.1. Mechanism of the cycloaddition reaction between phenylazide (1) and propiolaldehyde (2)

Only significant locations where noticeable changes in the electron population and valence basins occur are taken into account in this context's ELF analysis of a number of chosen points on the IRC of TS1's most favorable points (**Fig. 5**), the values of the basins are compiled in **Table 3** (**AZ-1** to **AZ-9**).

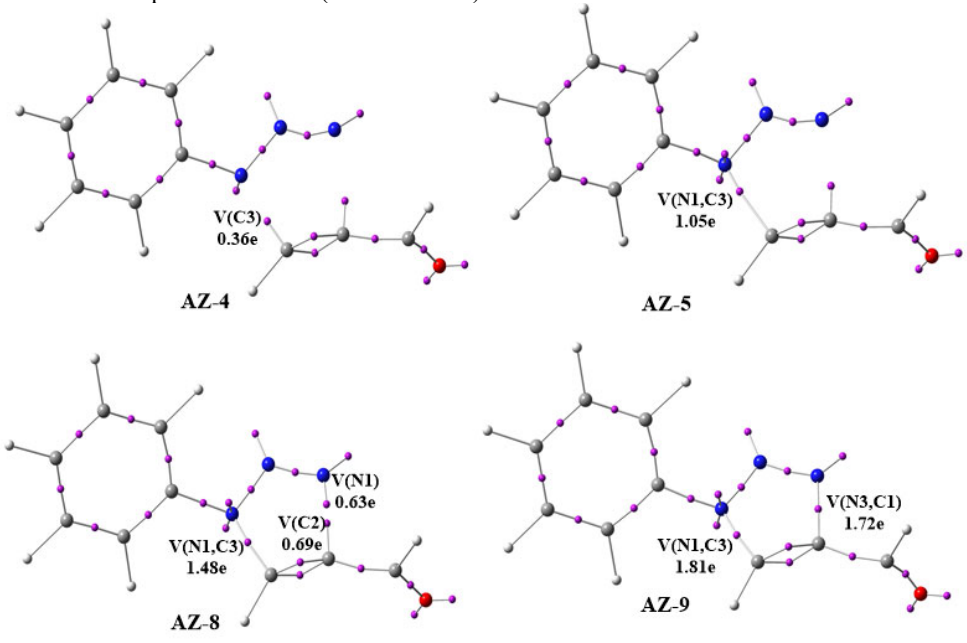

Fig. 5. Positions of the ELF valence attractors with populations for the AZ-4, AZ-5, AZ-8 and AZ-9 points involved in the IRC profile of TS-1

Table 3. ELF valence basin populations, distances of the forming bonds, of **TS1** and TS4, the selected structures of the IRC involved in the formation of the new single bonds along cycloaddition between phenylazide (**1**) with propiolaldehyde (**2**) and cycloaddition reaction between nitrile-oxide (**5**) and methyl-acrylate (**6**),. Electron populations are given in average number of electrons, e, and distances in angstroms, Å

	d(N3-C2)	d(N1-C3)	V(N1,N2)	V(N1)	V'(N1)	V(N2)	V(N2,N3)	V(N3)	V'(N3)	V(C2,C3)	V'(C2,C3)	V(C2)	V(C3)	V(N1,C3)	V(N3,C2)	***
AZ-1-TS-1	2.568	2.032	1.74	3.32	-	2.11	2.78	3.80	-	2.43	2.42	-	-		-	***
AZ-2	2.221	1.964	1.67	3.34	-	2.29	2.70	3.81	-	2.43	2.34	-	-		-	***
AZ-3	2.221	1.964	1.67	3.34	-	2.29	2.70	3.81	-	2.43	2.34	-	-		-	***
AZ-4	2.125	1.875	1.64	3.36	-	2.43	2.62	3.83	-	2.24	2.22	0.52	0.23		-	***
AZ-5	2.030	1.784	1.62	1.96	0.69	2.55	2.56	3.85	-	2.15	2.12	0.60	-	1.05	-	***
AZ-6	1.981	1.739	1.61	1.91	0.69	2.60	2.52	3.87	-	2.12	2.08	0.63	-	1.15	-	***
AZ-7	1.881	1.6529	1.60	1.81	0.68	2.70	2.45	3.53	0.38	2.07	2.02	0.67	-	1.32	-	***
AZ-8	1.775	1.5759	1.60	1.71	0.63	2.80	2.37	3.34	0.61	2.05	1.96	0.69	-	1.48	-	***
AZ-9	1.542	1.461	1.62	1.47	0.50	3.00	2.19	3.12	-	2.05	1.80	-	-	1.81	1.72	***
	d(O-C2)	**d(C-C3)**	**V(C4,N1)**	**V'(C4,N1)**	**V(N1)**	**V(C4)**	**V'(C4)**	**V(N1,O1)**	**V(O1)**	**V'(O1)**	**V(C2,C3)**	**V'(C2,C3)**	**V(C2)**	**V(C3)**	**V(C4,C3)**	**V(O1,C2)**
OX-1	3.069	3.138	2.87	2.62	-	0.66	-	1.53	2.92	2.78	1.70	1.69	-	-	-	-
OX-2-TS-4	2.440	2.172	1.75	1.48	1.96	1.34	-	1.41	2.82	2.79	3.17	-	-	-	-	-
OX-3	2.402	2.113	1.69	1.44	2.07	1.10	0.27	1.39	2.83	2.77	3.15	-	-	-	-	-
OX-4	2.365	2.053	1.93	1.42	2.16	0.76	0.38	1.37	2.82	2.78	2.87	-	-	0.25	-	-
OX-5	2.327	1.993	1.91	1.38	2.25	0.81	0.37	1.35	2.81	2.78	2.75	-	-	0.33	-	-
OX-6	2.288	1.934	1.89	1.37	2.32	-	0.36	1.32	2.80	2.79	2.66	-	-	-	1.25	-
OX-7	1.937	1.611	3.32	-	2.69	-	-	1.16	2.84	2.78	2.13	-	0.27	-	1.78	-
OX-8	1.807	1.573	3.28	-	2.76	-	-	1.09	2.96	2.72	2.06	-	0.32	-	1.85	-
OX-9	1.740	1.561	3.26	-	2.79	-	-	1.07	2.69	2.68	2.03	-	-	-	1.88	0.67
OX-10	1.607	1.540	3.22	-	2.85	-	-	1.00	2.60	2.60	1.98	-	-	-	1.92	0.94
OX-11	1.495	1.523	3.18	-	2.90	-	-	0.95	2.56	2.52	1.95	-	-	-	1.95	1.14

In the AZ-1 structure, there are three monosynaptic basins carried by the N1, N2 and N3 nitrogen atoms, with values of 3.32e, 3.11e and 3.80e respectively. Two bisynaptic basins located between (N1,N2) and (N2,N3), which respectively carry the following values: 1.74e and 2.78e, one also observes two bisynaptic basins located between the C2 and C3 carbons with a total value V(C2,C3)=4.85e. The two fragments, the azide and the alkene, move closer to each other, which influences the electronic distribution around the atoms, which becomes in the AZ-3 structure: V(N1)=3.34e, V(N2)=2.29e, V(N3)=3.81e, V(N1,N2)=1.67e, V(N2,N3)=2.70e and VT(C2,C3)=4.77e. In structure AZ-4 the appearance of two new monosynabtic basins carried by carbons C2 and C3 of value V(C2)=0.52e and V(C3)=0.23e.

In the AZ-5 structure, the monosynaptic basin V(N1= decomposes into three parts V(N1) with a value of 1.96e, V'(N1)=0.96e and the third part will be combined with V(C3) to form the first N1-C3 single bond with an electron population V(N1,C3)=1.05e. In the AZ-7 structure, the monosynaptic basin V(N3) d is decomposed into two basins V(N3) and V'(N3) respectively with values of 3.53e and 0.38e, these values become in the AZ-4 structure: V(N3)=0.34e and V'(N3)=0.61e. The monosynaptic pool V'(N3) will share its electron density with the monosynaptic pool V(C2) to form the second N3-C2 bond.

6.2. Mechanism of the cycloaddition reaction between nitrile oxide (5) and methyl acrylate (6)

The ELF analysis of certain selected points on the IRC of most favorable TS4's (**Fig. 6**) takes into account only major areas where noteworthy variations in the electron population and valence basins occur; the values of the basins are collected in **Table 3** (**OX-1** to OX-11).

During the cycloaddition reaction between nitrile oxide (**5**) and methyl acrylate (**6**), the electronic distribution in structure OX-1 is almost identical to that of the separate reactants. In structure OX-3 we have the appearance of two monosynaptic basins carried by the C4 carbon with values of V(C4)=1.10e and V'(C4)= 0.27e, these values will increase to V(C4)=0.81e and V'(C4)=0.37e in structure OX-5. In structure OX-4 we observe the appearance of a new monosynaptic carried by carbon C3 of value V(O3)=0.25e. In structure OX-6 the monosynaptic basins V(C4) and V(C3) will share their electron density to form the C3-C4 bond with an initial density V(C3,C4)=1.25e.

In structure OX-7 and OX-7, we have the apparition of a new monosynaptic carried by carbon C2 of value V(C3)=0.32e, this basin (V(C3)) will form the second O1-C2 bond with a part of monosynaptic basin of the oxygen atom. As a conclusion, the bonds are formed asynchronously in the reactions studied in this work.

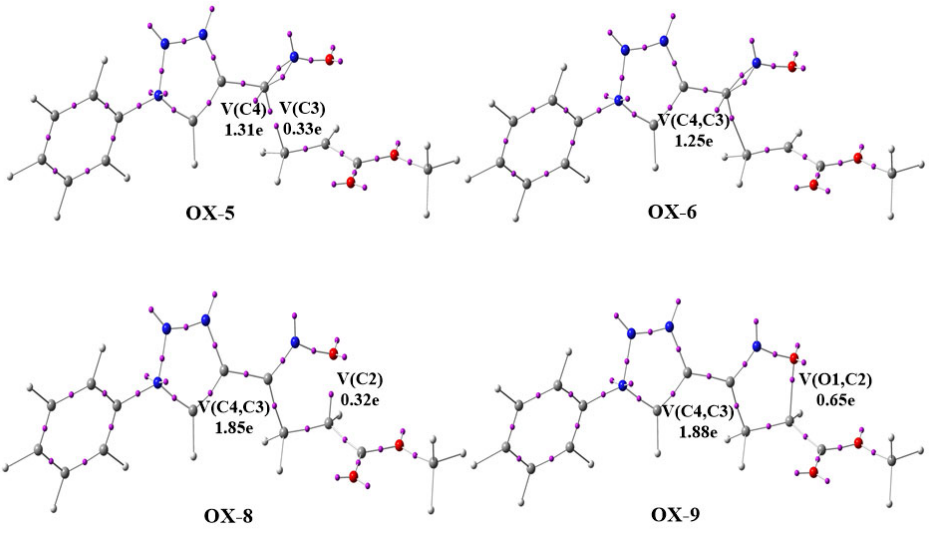

Fig. 6. Positions of the ELF valence attractors with populations for the OX-5, OX-6, OX-8 and OX-9 points involved in the IRC profile of TS-4

7. Docking analysis

Molecular docking is a modeling tool used in chemistry for researching at the relationships between ligands and proteins. In function to their chemical structure and energy potential, it allows for the prediction of the three-dimensional conformation of a molecular complex between a ligand and protein. It also enables the prediction of the affinity between a protein and a ligand, which can be helpful in the process of discovering drugs [43]. This section compares the antiviral activity of ribavirin to that of the antiviral products **3**, **4**, **7**, and **8**, which have been studied in relation to the crystal structures of the SARS-CoV-2 protease or the main COVID-19 protease (Mpro) in access numbers 6LU7. Biovia's Discover Studio 3.5 and PyMol 2.3 were employed to demonstrate the 2D and 3D molecular interactions of ligands 3, 4, 7 and 8 in the active sites of 6LU7 receptors. These interactions of 3, 4, 7, 8 and ribavirin are presented in **Fig. 7**, while the affinity is listed in **Table 4.**

Table 4. The affinity of **3**, **4**, **7**, **8** and ribavirin docked in COVID-19 main protease (6LU7)

Product	Affinity (kcal/mol)
3	-4.2
4	-4.8
7	-6.5
8	-6.4
Ribavirine	-6.2

The binding energies (kcal/mol) for the 6L7U crystal structure of the main protease of SARS-CoV-2 are in the order of -6.5 > -6.4> -6.2> -4.8>-4.2 kcal/mol for product 7 > product 8 > ribavirin > product 4 > product 3 >, respectfully. When compared to the standard antiviral drugs (ribavirin) and the other product under study, the product 7 > having triazoles and isoxazoles rings was found to have good antiviral activity, and we notice that its affinity is increased by the meta cyclization. The product 7 may therefore be the best antiviral medication, according to the results for the product 7 and ribavirin derivatives.

8. Conclusion

On the basis of B3LYP/6-31G(d,p), MEDT has used the concept to evaluate [3+2] cycloaddition reactions between 1 and 2 and 5 and 6, with the conclusion that 2 and 6 present as electrophiles for this reaction, **1** and **5** will participate as nucleophiles. Furthermore, the regioselectivity observed experimentally is perfectly confirmed by Parr function analysis. Moreover, these reactions are irreversible, thanks to their highly exergonic nature. ELF analysis of the most likely reaction trajectory asserts that this action occurs according to an uncoordinated mechanism, also, a docking investigation of products studied docked in Covid-19 major protease (6LU7) in comparison to Ribavirin was done; the findings indicate compounds 7 could serve as an antiviral drug.

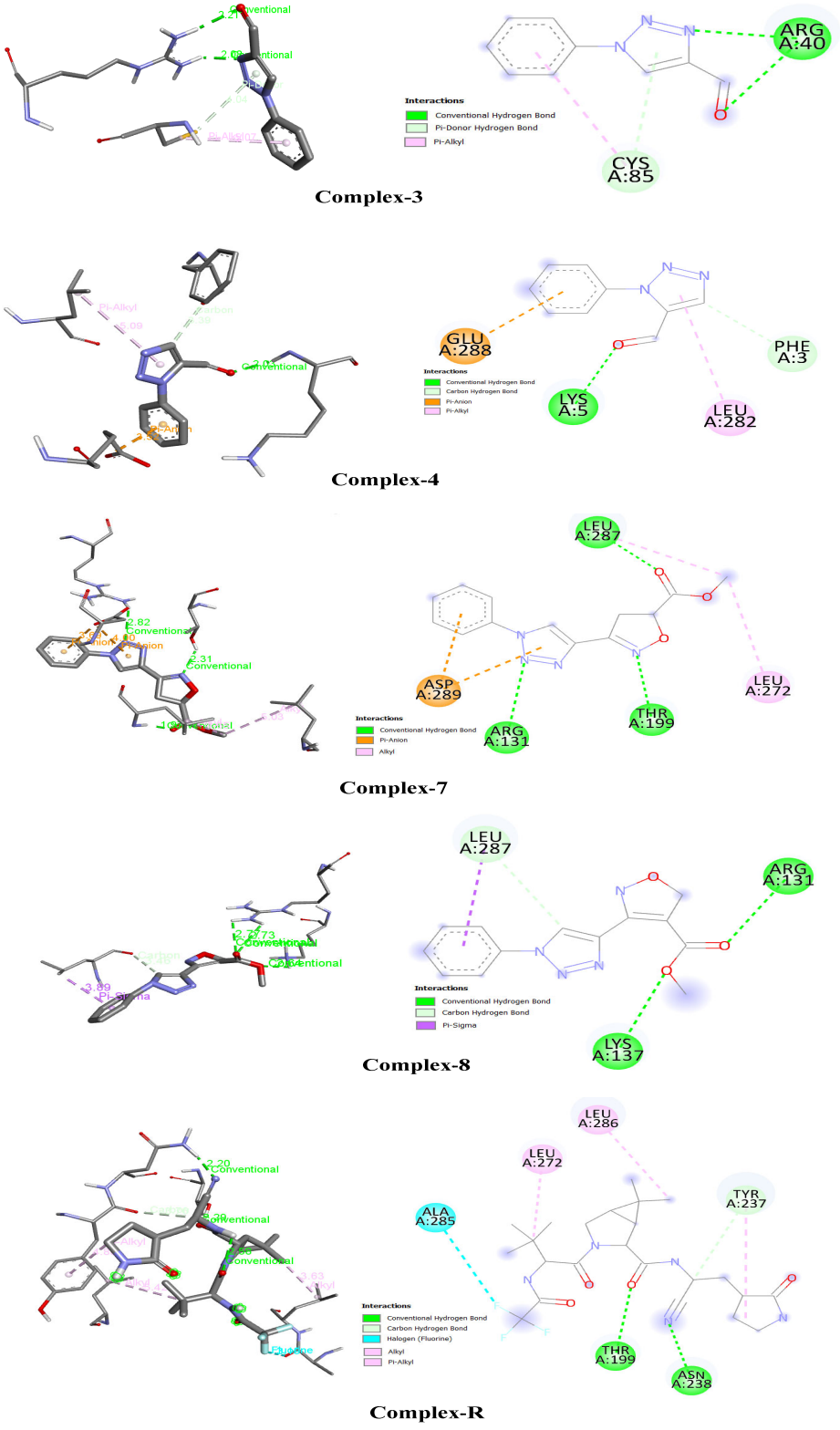

Fig. 7. 2-3-D-Visualizations of docking of 3, 4, 7, 8 docked in COVID-19 main protease (6LU7) compared to the Ribavirin.

Declaration of Competing Interest

The authors declare that they have no known competing financial interests or personal relationships that could have appeared to influence the work reported in this paper.

Declarations Funding

The authors received no specific funding for this work.

Ethics approval

The manuscript is prepared in compliance with the Ethics in Publishing Policy as described in the Guide for Authors.

References

1. Kras J., Sadowski M., Zawadzińska K., Nagatsky R., Woliński P., Kula K., Łapczuk A. (**2023**) Thermal [3+2] cycloaddition reactions as most universal way for the effective preparation of five-membered nitrogen containing heterocycles, Scientiae Radices, 2, 247-267. DOI: 10.58332/scirad2023v2i3a03
2. James Crowley D., David McMorra A. **(2012)** Coordination Chemistry: Exploiting 1,4-Disubstituted-1,2,3-Triazoles as Ligands, 28, 31-87 DOI:10.1007/7081_2011_67
3. Lauria A., Delisi R., Mingoia F., Terenzi A., Martorana A., Barone G., Almerico A.M., **(2014)** 1,2,3-Triazole in Heterocyclic Compounds, Endowed with Biological Activity, through 1,3-Dipolar Cycloadditions, Eur. J. Org. Chem 3289-3306 DOI: 10.1002/ejoc.201301695
4. Kawai H., Shibata N. **(2014)** Asymmetric Synthesis of Trifluoromethylated Dihydroazoles, The Chemical Record. 14, 1024-1040 DOI:10.1002/tcr.201402023
5. Zhu J., Jun M., Hong-zhi L., Chen Y., Hao-peng S. **(2018)** The recent progress of isoxazole in medicinal chemistry, Bioorganic and Medicinal Chemistry. 26(12), 3065-3075 DOI: 10.1016/j.bmc.2018.05.013.
6. Dadiboyena S., Jianping X., Ashton Hamme T. **(2006)** Isoxazoles, Electronics Properties, Annals of the New York Academy of Sciences. 1006, 235-251 DOI:10.1196/annals.1292.017
7. Domingo LR. **(2016)** Molecular Electron Density Theory: A Modern View of Reactivity in Organic Chemistry, Molecules. 21, 1319 DOI:10.3390/molecules21101319
8. El idrissi M., El Ghozlani M., Eşme A., Ríos-Gutiérrez M., Ouled Aitouna A., Salah M., El Abdallaoui H. E., Zeroual A., Mazoir N., Domingo LR. **(2021)** Mpro-SARS-CoV-2 Inhibitors and Various Chemical Reactivity of 1-Bromo- and 1-Chloro-4-vinylbenzene in [3 + 2] Cycloaddition Reactions, Organics, 2(1), 1-16 DOI:10.3390/org2010001
9. Zeroual A., Ríos-Gutiérrez M., M. El idrissi., Ouled Aitouna A., Salah M., El Abdallaoui H.E., Domingo LR. **(2020)** A molecular electron density theory investigation of the molecular mechanism, regioselectivity, stereoselectivity and chemoselectivity of cycloaddition reaction between acetonitrile N-oxide and 2,5-dimethyl-2H-[1,2,3]diazarsole, Theor Chem Acc 139 37 DOI:10.1007/s00214-020-2547-6
10. Zeroual A., Ríos-Gutiérrez M., Salah M., El Abdallaoui H.E., Domingo LR. **(2019)** An investigation of the molecular mechanism, chemoselectivity and regioselectivity of cycloaddition reaction between acetonitrile N-Oxide and 2,5-dimethyl-2H-[1,2,3]diazaphosphole: a MEDT study, J Chem Sci. 131, 75 DOI:10.1007/s12039-019-1656-z
11. Fryźlewicz A., Kącka-Zych A., Demchuk O. M., Mirosław B., Woliński P., Jasiński R., (**2021**) Green synthesis of nitrocyclopropane-type precursors of inhibitors for the maturation of fruits and vegetables via domino reactions of diazoalkanes with 2-nitroprop-1-ene, Journal of Cleaner Production, Volume 292, , 126079, https://doi.org/10.1016/j.jclepro.2021.126079.
12. Jasiński R., (2015) A stepwise, zwitterionic mechanism for the 1,3-dipolar cycloaddition between (Z)-C-4-methoxyphenyl-N-phenylnitrone and gem-chloronitroethene catalysed by 1-butyl-3-methylimidazolium ionic liquid cations, Tetrahedron Letters, Volume 56, Issue 3, 532-535, https://doi.org/10.1016/j.tetlet.2014.12.007.
13. Jasiński R., (2018) Competition between one-step and two-step mechanism in polar [3 + 2] cycloadditions of (Z)-C-(3,4,5-trimethoxyphenyl)-N-methyl-nitrone with (Z)-2-EWG-1-bromo-1-nitroethenes, Computational and Theoretical Chemistry, Volume 1125, 77-85, https://doi.org/10.1016/j.comptc.2018.01.009.
14. Zeroual A., Benharref A., El Hajbi A. **(2015)** Theoretical study of stereoselectivity of the [1+2] cycloaddition reaction between (1S,3R,8S)-2,2-dichloro-3,7,7,10-tetramethyltricyclo[6,4,0,$0^{1,3}$]dodec-9-ene and dibromocarbene using density functional theory (DFT). J. Mol Model. 21, 44 DOI:10.1007/s00894-015-2594-4
15. Barhoumi A., El idrissi M., Zeroual A. **(2021)** Theoretical study of the chemical reactivity of a class of trivalent phosphorus derivatives towards polyhaloalkanes: DFT study, J Mol Model. 27, 197 DOI:10.1007/s00894-021-04814-0
16. Barhoumi A., Ouled Aitouna A., Zeroual A., El idrissi M. **(2020)** Mechanistic Study of Hetero-Diels–Alder [4 + 2] Cycloaddition Reactions Between 2-Nitro-1H-Pyrrole and Isoprene, Chemistry Africa. 3, 901-909 DOI:10.1007/s42250-020-00187-8
17. Ameur S., Barhoumi A., Ríos-Gutiérrez M., Ouled Aitouna A., El Alaoui E.H., Mazoir N., Syed A., Zeroual A., Domingo L.R. **(2023)** A MEDT study of the mechanism and selectivity of the hetero-Diels–Alder reaction between 3-benzoylpyrrolo[1,2-c][1,4]-benzoxazine-1,2,4-trione and vinyl acetate, Chem. Heterocycl. Compd. 59(3), 165–170.
18. Zeroual A., Ríos-Gutiérrez M., El idrissi M., Domingo L.R. **(2019)** An MEDT Study of the Mechanism, Chemo- and Stereoselectivity of the Epoxidation Reaction of R-carvone with Peracetic Acid, RSC Advances Royal Society of Chemistry. 9, 28500-28509.

19. Zeroual A., M. Ríos-Gutiérrez, M. El idrissi, E.H. El Alaoui, L.R, Domingo, An MEDT study of the mechanism and selectivities of the [3+2] cycloaddition reaction of tomentosin with benzonitrile oxide, International Journal of Quantum Chemistry (2019) 1–9.
20. Aitouna A.O., Mazoir N., Zeroual A., Syed A., Bahkali Ali H., Elgorban A. M., Verma M., El idrissi M., · Jasiński R. **(2023)** Molecular docking, expounding the regiospecificity, stereoselectivity, and the mechanism of [5+2] cycloaddition reaction between ethereal ether and oxidopyrylium. J. Structural Chemistry. DOI:10.1007/s11224-023-02239-4
21. Smail T., Shafi S., Hyder I., Sidiq T., Khajuria A., Alam S.M., Halmuthur M.S.K. **(2015)** Design and Synthesis of Novel 1,2,3-Triazole- and 2-Isoxazoline-Based Bis-Heterocycles as Immune Potentiators, Arch. Pharm, Chem. Life Sci, 348, 796-807. DOI:10.1002/ardp.201400398.
22. McLean A.D., Chandler G.S. **(1980)** Contracted Gaussian-basis sets for molecular calculations. 1. 2nd row atoms, Z=11-18, J Chem Phys. 72, 5639-48 DOI:10.1063/1.438980
23. Krishnan R., Binkley J.S., Seeger R., **(1980)** Pople J.A. Self-Consistent Molecular Orbital Methods. 20. Basis set for correlated wave-functions, J Chem Phys. 72, 650-54. DOI:10.1063/1.438955
24. Gaussian 09, Revision A.02, M. J. Frisch et all, Gaussian, Inc., Wallingford CT**, (2009).**
25. Schlegel H.B. **(1982)** Optimization of equilibrium geometries and transition structures, J Comput Chem. 2 214-218. DOI:10.1002/wcms.34.
26. Schlegel H.B., Yarkony D.R. **(1994)** Modern Electronic Structure Theory, World Scientific Publishing, Singapore.
27. Tomasi J., Persico M. **(1994)** Molecular interactions in solution: an overview of Methods Based on continuous distributions of the solvent, Chem Rev. 94, 2027-2094 DOI:10.1021/cr00031a013
28. Cossi M., Barone V., Cammi R., Tomasi J. **(1996)** Ab initio study of solvated molecules: anew implementation of the polarizable continuum model, Chem Phys Lett. 255, 327-327 DOI:10.1016/0009-2614(96)00349-1.
29. Mennucci B., Cancès E., Tomasi J. **(1997)** Evaluation of solvent effects in isotropic and Anisotropic dielectrics and in ionic solutions with a unified integral equation method: theoretical bases, computational implementation, and numerical applications, J. Chem. Phys. 101, 10506-10517 DOI:10.1021/jp971959k
30. Barone V., Cossi M., Tomasi J. **(1998)** Geometry optimization of molecular structures insolution by the polarizable continuum model, J. Comput. Chem. 19 404-417.
31. Parr RG., Szentpaly LV., Liu S. **(1999)** Electrophilicity Index, J. Am. Chem. Soc. 121, 1922-1924 DOI:10.1021/ja983494x
32. Domingo LR., Pérez P. **(2011)** The nucleophilicity N index in organic chemistry. Org. Biomol. Chem. 9, 7168-7175 DOI:10.1039/C1OB05856H
33. Domingo LR., Perez P., Séaez JA. **(2013)** Understanding the local reactivity in polar organic reactions through electrophilic and nucleophilic Parr functions, RSC Adv. 3, 1486-1494. DOI:10.1039/C2RA22886F
34. Barhoumi A., Ourhriss N., Belghiti M. E., Chafi M., Syed A., laksh-manan Eswaramoorthy R., Verma M., Zeroual A., Zawadzińska K., Jasiński R. **(2023)** 3-Difluormethyl-5-carbomethoxy-2,4-pyrazole: Molecular mechanism of the formation and molecular docking study, Current Chemistry Letters. 12, 477–48 DOI:10.5267/j.ccl.2023.3.008.
35. Becke AD., Edgecombe KE. **(1990)** A simple measure of electron localization in atomic and molecular systems. J Chem Phys 92 5397-5403. DOI:10.1063/1.458517
36. Noury S., Krokidis X., Fuster F., Silvi B. **(1999)** Computational tools for the electron localizationfunction topological analysis, Comput Chem. 23, 597-604. DOI:10.1016/S0097-8485(99)00039-X.
37. Parr R.G., Yang W. **(1989)** Density-functional theory of atoms and molecules, Oxford University Press, New York.
38. Parr RG., Szentpály L.V., Liu S. **(1999)** Electrophilicity Index. J Am Chem Soc 121 1922-1924. DOI:10.1021/ja983494x
39. Domingo L.R., Aurell M J., Pérez P., Contreras R. **(2002)** Quantitative characterization of the global electrophilicity power of common diene/dienophile pairs in Diels–Alder reactions. Tetrahedron, 58 4417-4423. DOI:10.1016/S0040-4020(02)00410-6
40. Ríos-Gutiérrez M., Saz Sousa A., L.R. Domingo, **(2023)** Electrophilicity and nucleophilicity scales at different DFT computational levels. J Phys Org Chem. 36(7), e4503. DOI:10.1002/poc.4503.
41. Domingo L.R., Pérez P., Sáez J.A. **(2013)** Understanding the local reactivity in polar organic reactions through electrophilic and nucleophilic Parr function, RSC Advances. 3, 1486-1494. DOI:10.1039/C2RA22886F
42. Domingo L. R., Ríos-Gutiérrez M. (2023) A Useful Classification of Organic Reactions Based on the Flux of the Electron Density, Scientiae Radices, 2, 1-24, DOI: 10.58332/scirad2023v2i1a01
43. Zawadzińska K., Gostyński B. (**2023**) Nitrosubstituted analogs of isoxazolines and isoxazolidines: a surprising estimation of their biological activity via molecular docking. Scientiae Radices, 2, 25-46. DOI: 10.58332/scirad2023v2i1a02